## PAPER

Check for updates

# Development and characterization of a novel pH-responsive colorimetric indicator based on cellulose paper and polyvinyl alcohol loaded with alizarin for monitoring milk freshness

Satti Venu Gopala Kumari, †[a] Jibin Joseph,†[b] Kannan Pakshirajan[c] and G. Pugazhenthi *[de]

Milk is a highly perishable food product, and its quality is greatly influenced by storage and handling conditions. Consequently, there is a critical need for facile and reliable approaches, such as pH-responsive colorimetric indicators, to monitor milk freshness throughout the supply chain. In this context, the current study developed a novel and environmentally friendly colorimetric indicator by dip-coating cellulose paper (CP) with a polyvinyl alcohol (PVA)/alizarin solution for real-time monitoring of milk freshness. The developed CP/PVA/alizarin indicator exhibited a compact morphology without any phase separation, indicating excellent compatibility among its constituents. FTIR analysis disclosed intermolecular hydrogen bonding interactions between alizarin and the CP/PVA. The water solubility and swelling index of the indicator were observed to be 9.5 ± 0.6% and 77.2 ± 3.1%, respectively. In comparison with neat CP, the CP/PVA/alizarin indicator demonstrated an increase in crystallinity from 69 to 73%, an improvement in tensile strength from 5.2 ± 1.5 to 37.2 ± 1.1 MPa, and an enhancement in elongation at break from 2.6 ± 0.5 to 11.9 ± 1.1%. In addition, it exhibited distinct pH-sensitive color responses and excellent UV-blocking properties, with transmittance below 22.9%, 9%, and 3% in the UV-A, UV-B, and UV-C regions, respectively. It also showed a pronounced antioxidant activity of 68.3 ± 3.1%. Furthermore, the potential of CP/PVA/alizarin indicator in monitoring milk freshness was demonstrated through its perceivable color changes: pale brown for fresh milk (pH 6.5), orange-brown for semi-fresh milk (pH 5.5), and yellow-orange for spoiled milk (pH 4.5).

### Sustainability spotlight

The present study addressed the global challenge of food wastage and safety by developing a biodegradable, pH-responsive colorimetric indicator for real-time monitoring of milk freshness. Herein, the indicator fabricated using cellulose paper, polyvinyl alcohol, and alizarin enables visual detection of milk spoilage through distinct color transitions, mitigating reliance on predetermined expiration dates. Its eco-friendly composition, antioxidant activity, and UV-blocking properties contribute to reducing plastic waste and preserving food quality. Overall, this research aligns with the following UN Sustainable Development Goals (SDG): Zero Hunger (SDG2), Good Health and Well-being (SDG3), and Responsible Consumption and Production (SDG 12) by promoting sustainable food management and safer consumption practices.

## 1 Introduction

The quality and safety of food have a significant impact on public health and social well-being. Along the supply chain, food products are prone to spoilage due to a wide range of factors, *viz.*, microbial proliferation, physical stress, chemical reactions, and environmental conditions.[1] As per World Health Organization (WHO) reports, contaminated food consumption results in 420 000 deaths and 600 million cases of foodborne illness worldwide every year.[2] Conventionally, expiration or best-before dates are used to estimate food quality and determine recall timing. However, this passive information does not reflect the real-time condition of food, leaving consumers at risk

[a]Department of Chemical Engineering, National Institute of Technology Warangal, Warangal 506004, India

[b]Central Institute of Petrochemical Engineering and Technology, Institute of Petrochemicals Technology (IPT)-Kochi, Ernakulam 683501, Kerala, India

[c]Department of Biosciences and Bioengineering, Indian Institute of Technology Guwahati, Guwahati 781039, Assam, India

[d]Department of Chemical Engineering, Indian Institute of Technology Guwahati, Guwahati 781039, Assam, India. E-mail: pugal@iitg.ac.in; Tel: +91 361 258 2264

[e]Centre for Sustainable Polymers, Indian Institute of Technology Guwahati, Guwahati 781039, Assam, India

† Both authors made an equal contribution.

of foodborne illness even when expiration or best-before dates are followed. Additionally, early food recalls due to inaccurate/predetermined expiration dates are leading to a significant amount of food wastage worldwide and imposing substantial economic burdens on retailers and suppliers.[2,3] To address these challenges, the development of intelligent packaging systems capable of monitoring food freshness in real-time across the supply chain has emerged as one of the prominent areas of research in the food packaging field.[4–7]

Intelligent packaging systems are designed to sense and record internal and/or external changes in food products or in the packaging headspace and transduce these changes into signals that consumers can easily perceive. The intelligent packaging systems encompass a wide range of approaches, including microorganism indicators, humidity indicators, pH indicators, and time–temperature indicators.[8] Among these, indicators that exhibit colorimetric responses to pH variations arising from food spoilage have attracted considerable attention due to their ease of fabrication, cost-effectiveness, and facile and reliable visual transduction.[9,10] Such indicators typically comprise a synthetic polymer/biopolymer as a support and a pH-sensitive dye that reacts to chemicals released from the spoiled food. Nevertheless, to mitigate concerns related to plastic pollution and the potential migration of synthetic dyes into food products and their toxicological effects, recent studies have focused on exploring sustainable natural alternatives. Accordingly, biodegradable biopolymers such as chitosan, cellulose, polyvinyl alcohol (PVA), sodium alginate, κ-carrageenan, pectin, and starch, along with natural pH-sensitive dyes such as betalains, anthocyanins, curcumin, and alizarin, are being widely investigated.[9,11–13] For instance, gelatin/sodium alginate aerogels incorporated with cellulose nanofibers and *Echinacea angustifolia* encapsulated κ-carrageenan nanofibers have been reported for monitoring the freshness of fish fillets.[14] Likewise, pectin/betacyanin/UiO-66 packaging films and locust bean gum/κ-carrageenan/*Rosa canina* petal anthocyanin/chitosan nanofibrous mats were investigated for monitoring the freshness of pork and beef, respectively.[15,16] In another study, Khaledian *et al.* (2024) developed double-layer nanofibrous mats using starch/turnip peel anthocyanin and guar gum/cinnamaldehyde for monitoring lamb meat freshness and extending its shelf life.[17]

Alizarin, an anthraquinone dye obtained from the roots of *Rubia tinctorum* (madder plant), exhibits distinct pH-sensitive color changes, displaying yellow color in acidic, red in neutral, and purple in alkaline conditions. Its wide pH indicating range, non-toxicity, and good compatibility with biodegradable polymers, excellent antioxidant and UV-blocking properties, make it a versatile candidate for developing food freshness indicators.[18–20] Several studies reported in the literature demonstrated the potential of alizarin-loaded biopolymer-based colorimetric indicators for monitoring the freshness of seafood and meat. For instance, Ezati *et al.* (2019) investigated a cellulose/chitosan/alizarin indicator that exhibited a clear color change from yellow to purple in response to the spoilage of minced beef.[21] In another study, an antioxidant, antibacterial, and UV-resistant colorimetric indicator employing

chitosan and alizarin was reported to monitor shrimp freshness.[22] Likewise, cellulose/starch/alizarin[23] and konjac glucomannan/curcumin/alizarin[24] indicators showed clear color transitions in response to the spoilage of fish fillets and pork, respectively. As a supporting matrix, cellulose paper (CP) offers several advantages, including biodegradability, low cost, hydroxy groups that enable chemical modification, and a porous structure that facilitates rapid absorption and immobilization of dyes.[25,26] However, direct coating of dye onto CP yields an indicator with poor mechanical strength and poor dye retention, which compromises its stability and reliability.[26] To address these limitations, recent studies have advocated the use of polymer/alizarin composite solutions, based on biopolymers such as starch, chitosan, and PVA, for coating CP substrates to enhance mechanical integrity and improve dye retention.[21,23,27]

Milk, a globally consumed food product, is highly prone to spoilage due to its rich nutrient composition, which supports the proliferation of microorganisms that cause spoilage. Freshness of milk can be assessed using parameters such as bacterial count, protein concentration, odor, and pH.[4] Conventionally, microbial and chemical tests are conducted for milk at the company level before packaging. However, such quality assessments are absent after the product is delivered at the distributor/consumer level.[28] Therefore, there is a need to develop facile and sensitive technologies capable of monitoring milk freshness across the supply chain. While alizarin-loaded biopolymer indicators have been widely investigated for monitoring the freshness of meat and seafood, exhibiting excellent pH-responsive colorimetric behavior, their application in milk quality assessment remains largely unexplored.[18,20,22,29] To the best of our knowledge, no study has reported the development of a pH-responsive colorimetric indicator based on a combination of CP, PVA, and alizarin for evaluating milk freshness. To address this gap, in the present study, a novel pH-responsive colorimetric indicator was developed by dip-coating CP with a PVA/alizarin solution and tested for monitoring milk freshness. Herein, PVA was opted for its excellent film-forming ability, tensile properties, biodegradability, and biocompatibility.[30] The morphology and functional group analysis of the prepared CP/PVA/alizarin indicator were carried out using FESEM and FTIR instruments, respectively. In addition, its water solubility, swelling index, structural, optical, tensile, and antioxidant properties were evaluated. The colorimetric response of the indicator was assessed over a pH range of 2–11, and its potential to distinguish fresh, semi-fresh, and spoiled milk was demonstrated.

## 2 Materials and methods

### 2.1. Materials

2,2-Diphenyl-1-picrylhydrazyl hydrate (DPPH, ≥90%), alizarin (97% dye content), and lactic acid (≥85% in $H_2O$) were purchased from Sigma-Aldrich Co. Ltd [India]. Polyvinyl alcohol (PVA) (molecular weight: 115 kDa, synthesis grade) was supplied by Loba Chemie Pvt. Ltd [India]. HCl (36.5–38%), NaOH (>97%), and cellulose papers (Whatman®, grade 1) were procured from Merck Specialties Pvt. Ltd [India]. Methanol

(>98.8%) was supplied by Finar Ltd [India]. Fresh buffalo milk was purchased from a local dairy farm in Guwahati, India. All chemicals were used as received without further purification. Water used in all experiments was obtained from an in-house Millipore purification system (Millipore Elix-3, USA).

## 2.2. Fabrication of colorimetric indicator

Firstly, 5 g of PVA was dissolved in 50 mL of Millipore water by mixing with a magnetic stirrer at 95 °C and 300 rpm for 6 h.[30] Subsequently, 0.05 g of alizarin was added to the PVA solution and mixed at 700 rpm and room temperature for 1 h. Afterward, the cellulose paper (CP) (4 cm × 4 cm) was dip-coated in the PVA/alizarin solution for 30 s and dried at 80 °C for 24 h in a hot-air oven to obtain the CP/PVA/alizarin colorimetric indicator. Herein, the alizarin loading rate was fixed based on preliminary experiments with varying alizarin concentrations. These experiments demonstrated that 0.1% w/v of alizarin (with respect to the PVA solution) was the minimum concentration capable of producing a distinct and visually perceptible colorimetric response for the indicator across the tested pH range (2–11). For comparison, CP (4 cm × 4 cm) coated only with a PVA solution, referred to as CP/PVA, was also prepared. A schematic depicting the steps involved in the fabrication of the CP/PVA/alizarin indicator is presented in Fig. 1.

## 2.3. Characterization

**2.3.1. Physicochemical properties.** Functional group analysis of alizarin, CP, CP/PVA, and CP/PVA/alizarin samples was carried out in the wavenumber range of 400–4000 cm$^{-1}$ using Fourier transform infrared (FTIR) spectroscopy (Shimadzu, IRAffinity-1, Japan). Surface morphology of various CP-based samples was analyzed using a Field emission scanning electron microscope (FESEM) (Zeiss, Sigma 300, Germany). The X-ray diffraction (XRD) spectra of CP, CP/PVA, and CP/PVA/alizarin were recorded in the $2\theta$ range of 5–80° employing an X-ray diffractometer (Rigaku, Micromax-007HF, Japan).

**2.3.2. Water solubility and swelling index.** The water solubility and swelling index of the CP, CP/PVA, and CP/PVA/alizarin samples were measured according to the procedure described in the literature,[21] with slight modifications. Each sample was initially dried in a hot air oven at 100 °C for 24 h, and the dry mass was recorded as $m_1$. The dried samples were then incubated individually in 50 mL of Millipore water for 24 h. After incubation, excess surface water on the samples was gently removed, and the wet mass ($m_2$) was recorded. Subsequently, the samples were re-dried in a hot air oven at 100 °C until constant weight was achieved, and the final dry mass was recorded as $m_3$. The water solubility and swelling index of the samples were subsequently estimated using eqn (1) and (2), respectively.[21,31]

$$\text{Water solubility}(\%) = \frac{m_1 - m_3}{m_1} \times 100 \tag{1}$$

$$\text{Swelling index}(\%) = \frac{m_2 - m_1}{m_1} \times 100 \tag{2}$$

The experiments were repeated in triplicate, and the results were reported as mean ± standard deviation. One-way ANOVA followed by Tukey's post hoc test was performed using Origin™ Pro 9.0 software to assess statistical significance ($p < 0.05$).

**2.3.3. Tensile and optical properties.** Tensile properties of CP, CP/PVA, and CP/PVA/alizarin samples were evaluated using an Electromechanical universal testing machine (Z005TN, Zwick Roell, USA) adopting ASTM D882-12 standard. At least three samples of each type were tested, and the results are presented as mean ± standard deviation. Statistical analysis of the tensile test results was conducted using one-way ANOVA, followed by Tukey's post hoc test ($p < 0.05$), employing Origin™ Pro 9.0 software. The transmittance spectra of various CP-based samples in the wavelength range of 200–700 nm were measured using a UV-visible spectrophotometer (Shimadzu, UV-2600, Singapore), with a BaSO$_4$-coated plate employed as the reference. Subsequently, opacity values of various CP-based samples were calculated using eqn (3).[32]

$$\text{Opacity value} = \frac{-\log(T_{600})}{k} \tag{3}$$

Herein, $k$ is the average sample thickness (mm), and $T_{600}$ is the fractional transmission at 600 nm.

**2.3.4. Antioxidant activity.** DPPH radical scavenging assay was adopted to determine the antioxidant activity of CP, CP/PVA, and CP/PVA/alizarin samples.[31,33] For the test, each sample was incubated in 10 mL of methanolic DPPH solution (0.1 mM) for 30 min in the dark at room temperature. After incubation, the absorbance of the resulting solution ($A_{sp}$) was
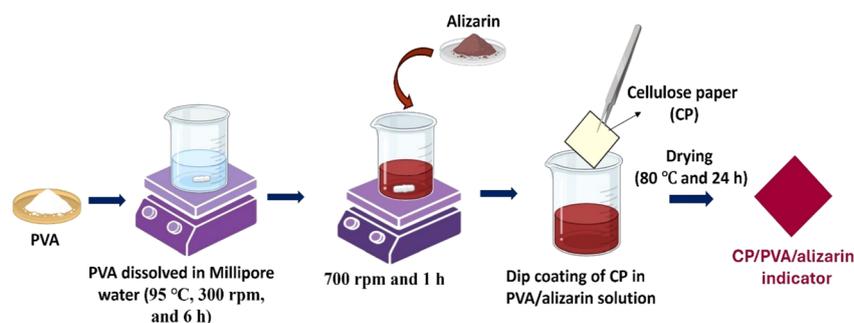


**Fig. 1** Schematic depicting the fabrication of CP/PVA/alizarin indicator.

measured at 517 nm using a UV-visible spectrophotometer (Shimadzu, UV-2600, Singapore). A control study was carried out following the same experimental procedure using a blank methanolic DPPH solution, and the absorbance was recorded as $A_{ct}$. Subsequently, the antioxidant activity of the samples was calculated using eqn (4).[31,33]

$$\text{Antioxidant activity}(\%) = \frac{A_{ct} - A_{sp}}{A_{ct}} \times 100 \tag{4}$$

**2.3.5. Colorimetric characteristics of CP/PVA/alizarin.** To evaluate the colorimetric response of CP/PVA/alizarin indicator under different pH conditions, buffer solutions with pH values ranging from 2 to 11 were prepared using NaOH, HCl, and Millipore water, employing a pH meter (Eutech, India).[23] The CP/PVA/alizarin samples were incubated in the corresponding pH solutions for 2 min and subsequently photographed. In addition, the color parameters, *viz.*, $L^*$ (dark/light), $a^*$ (red/green), and $b^*$ (yellow/blue) of the indicator were measured using a color spectrophotometer (Sensegood, India). Finally, the color difference with respect to the as-prepared CP/PVA/alizarin indicator (control) is calculated using eqn (5).[23]

$$\Delta E = \sqrt{\left(L^*_{sample} - L^*_{control}\right)^2 + \left(a^*_{sample} - a^*_{control}\right)^2 + \left(b^*_{sample} - b^*_{control}\right)^2} \tag{5}$$

### 2.4. Application of colorimetric indicator in monitoring milk freshness

The performance of the CP/PVA/alizarin indicator to differentiate fresh, semi-fresh, and spoiled milk was evaluated by adapting the experimental procedure described in the literature.[4] For the evaluation, fresh milk (pH 6.5) was used as the control, while semi-fresh and spoiled conditions were simulated by adjusting the pH of milk to 5.5 and 4.5, respectively, through dropwise addition of lactic acid. The CP/PVA/alizarin indicators were incubated individually in 10 mL of milk samples of pH 6.5, 5.5, and 4.5 for 5 min. Following the incubation, the indicators were retrieved, photographed, and subjected to colorimetric analysis using a color spectrophotometer (Sensegood, India).

## 3 Results and discussion

### 3.1. Physicochemical properties

**3.1.1. FTIR analysis.** FTIR analysis was conducted on CP, CP/PVA, alizarin powder, and CP/PVA/alizarin to evaluate the nature of interactions among the constituents of the indicator (Fig. 2). The functional group assignments for the transmittance peaks are summarized in Table 1. In the FTIR spectrum of CP, the broad transmittance peak corresponding to O–H stretching was observed at 3347 cm$^{-1}$ (Table 1). This peak shifted to 3239 cm$^{-1}$ in the FTIR spectrum of CP/PVA, indicating the hydrogen bonding interactions between CP and PVA.[23] The FTIR spectra of CP as well as CP/PVA showed C–H
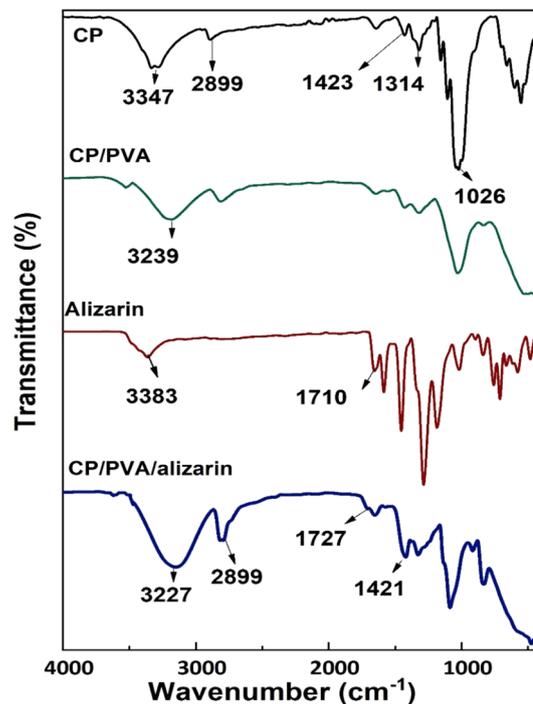


**Fig. 2** FTIR spectra of CP, CP/PVA, alizarin, and CP/PVA/alizarin.

stretching peaks at 2899 cm$^{-1}$, along with a small peak at 1652 cm$^{-1}$, attributed to the surface adsorbed water. Additionally, the characteristic peaks corresponding to symmetric CH$_2$ bending, C–H bending, C–O–C stretching, and C–O stretching were observed at 1423, 1314, 1137, and 1026 cm$^{-1}$, respectively, for both CP and CP/PVA.[21,34] The FTIR spectrum of alizarin powder showed a transmittance peak at 3383 cm$^{-1}$, corresponding to the –OH group (Table 1). Additionally, the transmittance peak associated with the C=O group was observed at 1710 cm$^{-1}$, while the peaks for aromatic C=C bonds were noticed in the wavenumber range of 1580–1300 cm$^{-1}$.[35,36] The

**Table 1** Functional group assignments for the transmittance peaks

| Sample | Wavenumber (cm$^{-1}$) | Peak assignment |
|---|---|---|
| CP and CP/PVA | 3347 | O–H stretching |
| | 3239 | O–H stretching |
| | 2899 | C–H stretching |
| | 1652 | O–H bending vibration of surface-adsorbed water |
| | 1423 | CH$_2$ bending |
| | 1314 | C–H bending |
| | 1137 | C–O–C stretching |
| | 1026 | C–O stretching |
| Alizarin | 3383 | O–H stretching |
| | 1710 | C=O group |
| | 1580–1300 | C=C bonds |
| CP/PVA/alizarin | 3227 | O–H stretching |
| | 2899 | C–H stretching |
| | 1727 | C=O group |
| | 1421 | CH$_2$ bending |

C=O stretching band, observed at 1710 cm$^{-1}$ in the FTIR spectrum of alizarin powder, shifted to 1727 cm$^{-1}$ in the FTIR spectrum of CP/PVA/alizarin. Likewise, the O–H stretching band noticed at 3239 cm$^{-1}$ for CP/PVA shifted to 3227 cm$^{-1}$ for CP/PVA/alizarin. The remaining characteristic peaks of CP/PVA and alizarin appeared in the FTIR spectrum of CP/PVA/alizarin without any significant shift/modification. This result indicates that alizarin primarily interacts with the CP/PVA matrix through hydrogen bonding involving its –OH and C=O groups. A similar observation regarding intermolecular hydrogen bonding interaction between alizarin and CP/chitosan matrix was reported in the literature.[21]

**3.1.2. Morphological and structural properties.** The surface morphology of CP, CP/PVA, and CP/PVA/alizarin is analyzed by FESEM. Neat CP exhibited a heterogeneous porous morphology characterized by randomly oriented micro and nanofibrils and inter-fiber voids (Fig. 3a and a'). Coating with PVA yielded a smooth and compact surface for CP/PVA, effectively covering the pores of CP and showing no phase separation, indicating good compatibility between CP and PVA (Fig. 3b and b'). The FESEM image of CP/PVA/alizarin showed a compact morphology similar to that of CP/PVA, with no phase separation or aggregate formation, implying excellent compatibility and uniform dispersion of alizarin in the PVA-based coating (Fig. 3c and c'). The structural properties of CP, CP/PVA, and CP/PVA/alizarin are analyzed by XRD analysis (Fig. 3d). The crystallinity values of these samples were calculated by dividing the total area under crystalline peaks by the cumulative area of all the peaks present in their respective XRD spectra.[30] From Fig. 3d, it can be observed that the neat CP exhibited diffraction peaks at 14.5°, 16.5°, 22.6°, and 34.3° corresponding to (1 $\bar{1}$ 0), (1 1 0), (2 0 0), and (0 0 4) planes of cellulose I, respectively.[37] The CP/PVA showed all the characteristic peaks of CP, along with an additional diffraction peak at $2\theta = 19.3°$, attributable to the (1 0 $\bar{1}$) plane of the orthorhombic lattice of PVA.[30] The XRD spectrum of CP/PVA/alizarin also exhibited all the peaks observed for CP/PVA, with no additional peaks corresponding to alizarin, likely due to its low loading. These results suggest that the crystal structure of the CP substrate was not affected by the PVA or PVA/alizarin coating. Nevertheless, the crystallinity increased from 69% for CP to 72% and 73% for CP/PVA and CP/PVA/alizarin, respectively. This increase in crystallinity can be attributed to hydrogen-bonding interactions between the CP substrate and the coating materials, discussed earlier in Section 3.1.1. A similar observation was reported in the literature, where coating CP with a PVA/polyethylene oxide blend resulted in increased crystallinity.[6]

## 3.2. Water solubility and swelling index

Water solubility and swelling index results of CP, CP/PVA, and CP/PVA/alizarin are presented in Fig. 4. Herein, water solubility indicates the extent of polymer matrix dissolution and/or dye leaching under humid conditions.[10,12] On the other hand, the swelling index measures the water absorption and retention
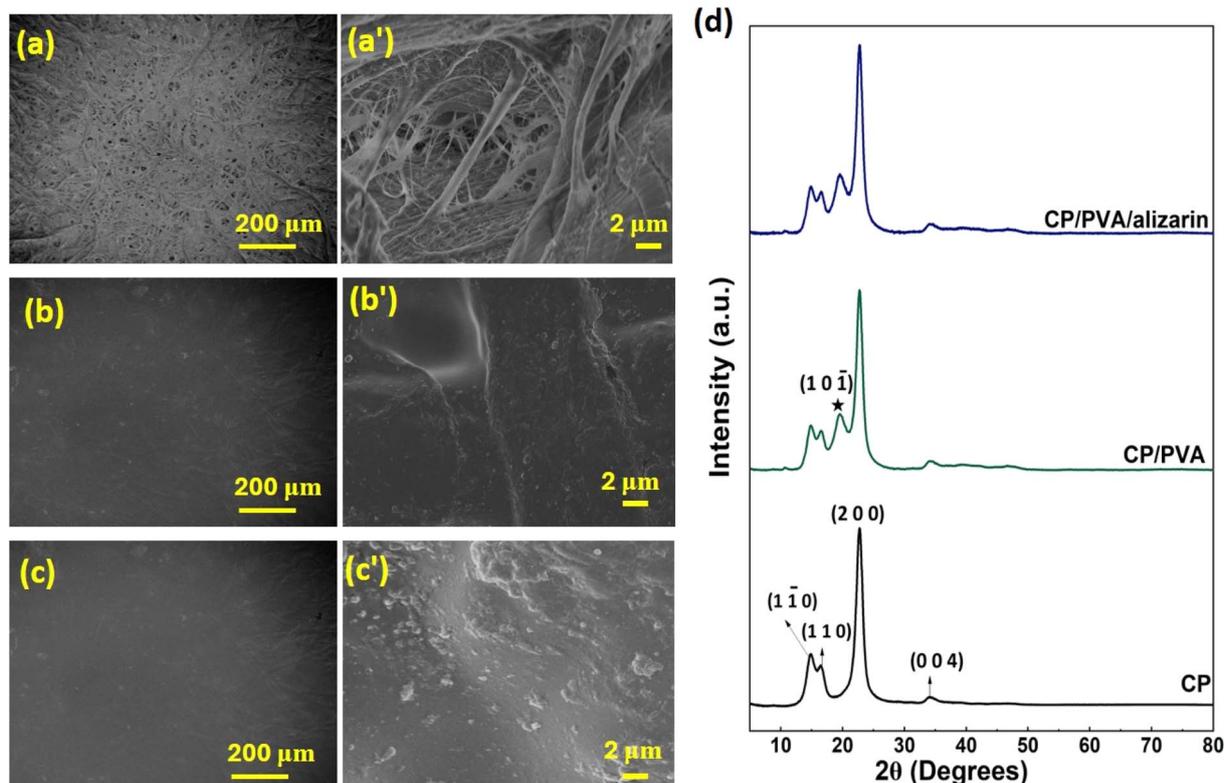


**Fig. 3** Lower (a–c) and higher (a'–c') magnification FESEM images of CP, CP/PVA, and CP/PVA/alizarin, respectively (d) XRD spectra of CP, CP/PVA, and CP/PVA/alizarin (diffraction peak of PVA is marked using ★ symbol).
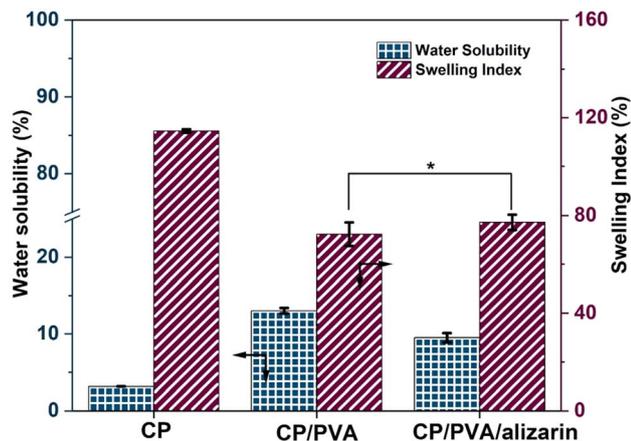
Fig. 4 Water solubility and swelling index of CP, CP/PVA, and CP/PVA/alizarin (*$p > 0.05$: indicates no significant difference).



Fig. 5 Tensile properties of CP, CP/PVA, and CP/PVA/alizarin (*$p > 0.05$: indicates no significant difference).

capacity of the material, which directly influences dye mobility and colorimetric response. For colorimetric indicators, low water solubility is crucial to avoid dye leaching and maintain its functional stability throughout storage and application. Likewise, a moderate swelling index is required to enable adequate water uptake for a rapid and sensitive colorimetric response.[10,12] The water solubility and swelling index of CP are $3.1 \pm 0.1$ and $114.5 \pm 0.6\%$, respectively. Upon coating CP with PVA, the water solubility increased to $13.1 \pm 0.4\%$, which is attributable to the hydrophilic nature of PVA.[38] In contrast, the CP/PVA/alizarin sample exhibited a reduced water solubility of $9.5 \pm 0.6\%$. This is due to the hydrophobicity of alizarin and hydrogen bonding interactions between the polymer chains and alizarin, which decreases the number of free hydrophilic groups in the polymer matrix.[23] Considering the swelling index, coating CP with PVA reduced its swelling index to $72.2 \pm 4.8\%$, approximately 1.6-fold lower than that of neat CP. This reduction can be attributed to the formation of a dense semi-crystalline PVA barrier layer on the CP surface, and the limited availability of free hydrophilic groups, both of which restrict water absorption and polymer chain expansion.[23] Meanwhile, no significant change in swelling index is observed for CP/PVA/alizarin ($77.2 \pm 3.1\%$) compared to CP/PVA. Similar findings were reported in the literature,[23] wherein coating CP with starch resulted in a reduced swelling index, while the incorporation of alizarin showed no significant influence on the swelling index value.

### 3.3. Tensile and optical properties

Tensile properties, *viz.*, tensile strength and elongation at break, are critical parameters that determine the robustness of the colorimetric indicator when incorporated into packaging systems.[39] Therefore, these properties were evaluated for CP, CP/PVA, and CP/PVA/alizarin to assess the influence of coating materials (Fig. 5). As can be observed in Fig. 5, CP exhibited tensile strength and elongation at break of $5.2 \pm 1.5$ MPa and $2.6 \pm 0.5\%$, respectively. Compared to neat CP, a remarkable 6.7-fold increment in tensile strength and 4.6-fold increment in elongation at break were observed for CP/PVA. Herein, the
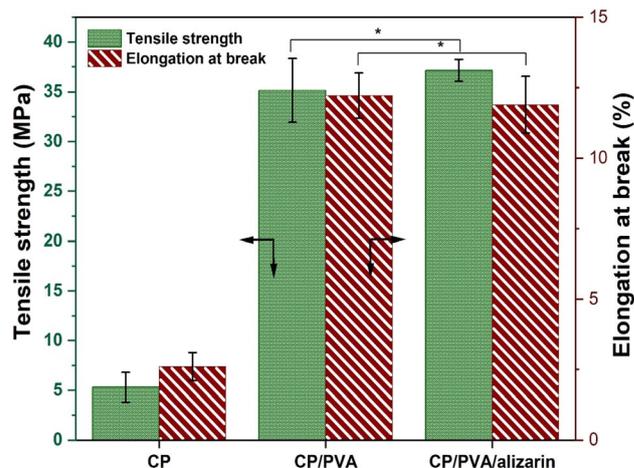
significant enhancement in tensile strength of CP/PVA can be attributed to the filling of voids between cellulose fibers by the PVA and the hydrogen bonding interactions between cellulose and PVA molecules. These hydrogen bonds act as physical crosslinks at the molecular level, effectively binding the cellulose fibers and PVA polymer chains, thereby allowing efficient stress distribution in the CP/PVA.[39,40] On the other hand, the increment in elongation at break of CP/PVA is due to the inherent high flexibility of PVA, which imparts toughness to the coated substrate, allowing greater deformation before failure.[7,30] A similar trend of increase in tensile strength and elongation at break was reported in the literature for CP coated with chitosan[39] and CP coated with chitosan/carboxymethyl cellulose.[7] Notably, CP/PVA/alizarin indicator exhibited tensile strength and elongation at break of $37.2 \pm 1.1$ MPa and $11.9 \pm 1.1\%$, respectively, which were not significantly different from those of CP/PVA. This observation is consistent with the findings reported by Huang *et al.* (2019), wherein the incorporation of *Arnebia euchroma* root extract showed no significant effect on the tensile properties of agar-based colorimetric indicator.[11]

The UV-visible light transmittance spectra of CP, CP/PVA, and CP/PVA/alizarin are shown in Fig. 6. Food packaging materials require UV-blocking properties to prevent nutrient degradation, discoloration, and undesirable alterations in the taste and texture of food products caused by direct exposure to ultraviolet radiation. Conversely, the requirement for visible-light transmittance depends on the type of food and its sensitivity to light. Products such as fruits, vegetables, and bakery items benefit from packaging with high transparency materials. In contrast, light-sensitive products, including nuts, milk, and vegetable oils, require packaging with low transparency.[9,41] From Fig. 6, it can be observed that neat CP showed greater than 92% transmittance in the visible region (400–700 nm) and approximately 91, 80, and 71% transmittance in the UV-A (315–400 nm), UV-B (280–315 nm), and UV-C (280–200 nm) regions, respectively. Coating the CP substrate with PVA resulted in
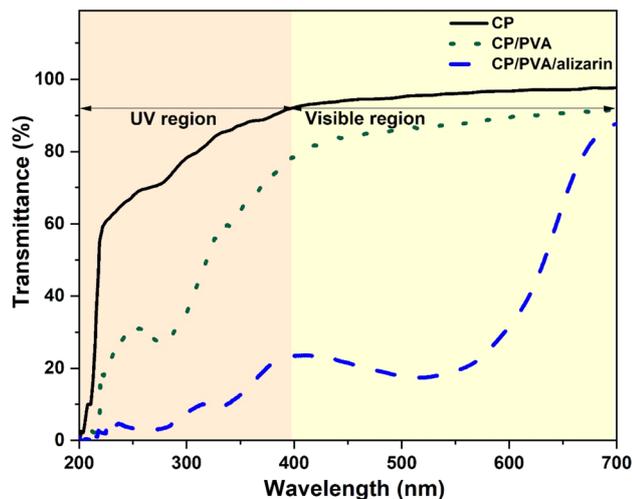
**Fig. 6** UV–visible light transmittance spectra of CP, CP/PVA, and CP/PVA/alizarin.



**Fig. 7** (a) Antioxidant activity of CP, CP/PVA, and CP/PVA/alizarin, and (b) DPPH radical scavenging reaction of alizarin.

a significant decrease in UV light transmission to approximately 77%, 46%, and 27% in the UV-A, UV-B, and UV-C regions, respectively. This reduction can be attributed to the scattering of light at the interface of PVA crystallites. The incorporation of alizarin into the PVA-based coating further decreased UV light transmission to 22%, 9%, and 3% in the UV-A, UV-B, and UV-C regions, respectively. This pronounced UV-blocking effect of CP/PVA/alizarin is primarily ascribed to the absorption of UV light by the alizarin.[23] Similar observations regarding the UV blocking properties of alizarin-loaded colorimetric indicator were reported earlier in the literature.[9,23] The opacity values of CP, CP/PVA, and CP/PVA/alizarin are obtained as 0.07, 0.27, and 2.3 A. mm$^{-1}$, respectively. Higher opacity value of CP/PVA/alizarin compared to CP indicates its lower transparency to visible light.[32] Thus, the enhanced UV and visible light barrier properties of CP/PVA/alizarin indicate its potential for packaging light-sensitive products, such as milk.

### 3.4. Antioxidant activity

Antioxidant activity is a vital characteristic required for packaging materials to extend the shelf-life of food products by preventing/reducing oxidative degradation, which otherwise results in undesirable effects like off-flavors, rancidity, and discoloration in food.[42] As discussed in detail later in Section 3.6, the CP/PVA/alizarin indicator is designed to be integrated into conventional milk packaging in such a way that it maintains direct contact with the milk while remaining visible to both consumers and automated cameras. In this context, the antioxidant activity of the indicator was evaluated to determine whether the incorporated alizarin could provide additional benefits for extending milk shelf-life beyond pH-responsive spoilage sensing.[22] The results of the antioxidant activity assay of CP, CP/PVA, and CP/PVA/alizarin are presented in Fig. 7a. As can be seen in Fig. 7a, CP and CP/PVA showed negligible antioxidant activity, consistent with previous studies that reported cellulose and PVA lack intrinsic
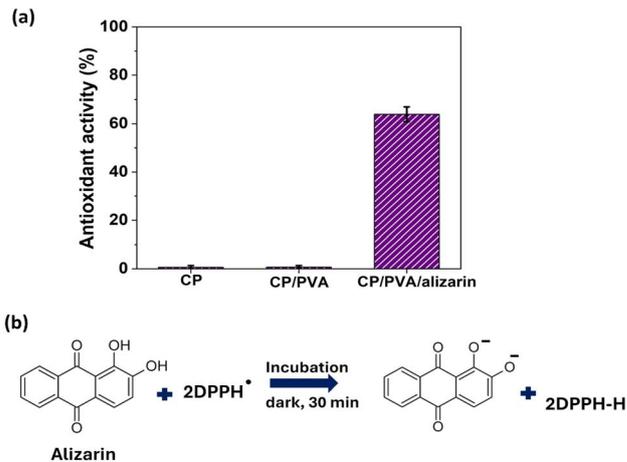
antioxidant properties.[5,43] In contrast, CP/PVA/alizarin exhibited a pronounced antioxidant activity of 68.3 ± 3.1%, demonstrating the effectiveness of alizarin as a natural antioxidant. Herein, the antioxidant activity of alizarin can be ascribed to its ability to donate hydrogen atoms from its phenolic hydroxyl groups to neutralize DPPH free radicals (Fig. 7b).[9] Moreover, this observation is in good agreement with the study reported by Ezati et al. (2020), wherein the antioxidant activity of chitosan-based films increased from 10 to 40% with the incorporation of 1 wt% alizarin.[22]

### 3.5. Colorimetric characteristics of CP/PVA/alizarin indicator

The color response of CP/PVA/alizarin indicator at varied pH conditions from 2 to 11 is shown in Fig. 8a. The indicator exhibited a yellow color at pH 2, which progressively shifted to a yellow-orange color in the pH range of 3–5. At pH 6, it developed a pale brown color that deepened to reddish-brown at pH 7–8. Thereafter, at pH 9, the color of the indicator transitioned to brownish-purple, which intensified to a bright purple in the pH range of 10–11. These pH-responsive color transitions of the CP/PVA/alizarin indicator can be attributed to the protonation and deprotonation of the phenolic hydroxyl groups of the anthraquinone ring in alizarin (Fig. 8b). Under acidic conditions, alizarin remains predominantly in its neutral form, with both hydroxyl groups protonated. At neutral pH, one hydroxyl group loses a proton, leading to a mono-anionic form, whereas under alkaline conditions, both hydroxyl groups are deprotonated, yielding a dianionic form. These structural transitions modulate electron delocalization and intermolecular hydrogen bonding in alizarin, which in turn influences the chromatic response of the indicator across different pH environments.[29,44] To quantitatively assess the color variations, the colorimetric parameters ($L*$, $a*$, $b*$ and $\Delta E$) of the CP/PVA/alizarin indicator at different pH conditions in the range of 2–11 were determined (Fig. 8c). As can be observed in Fig. 8c, the $L*$ value, indicating brightness/
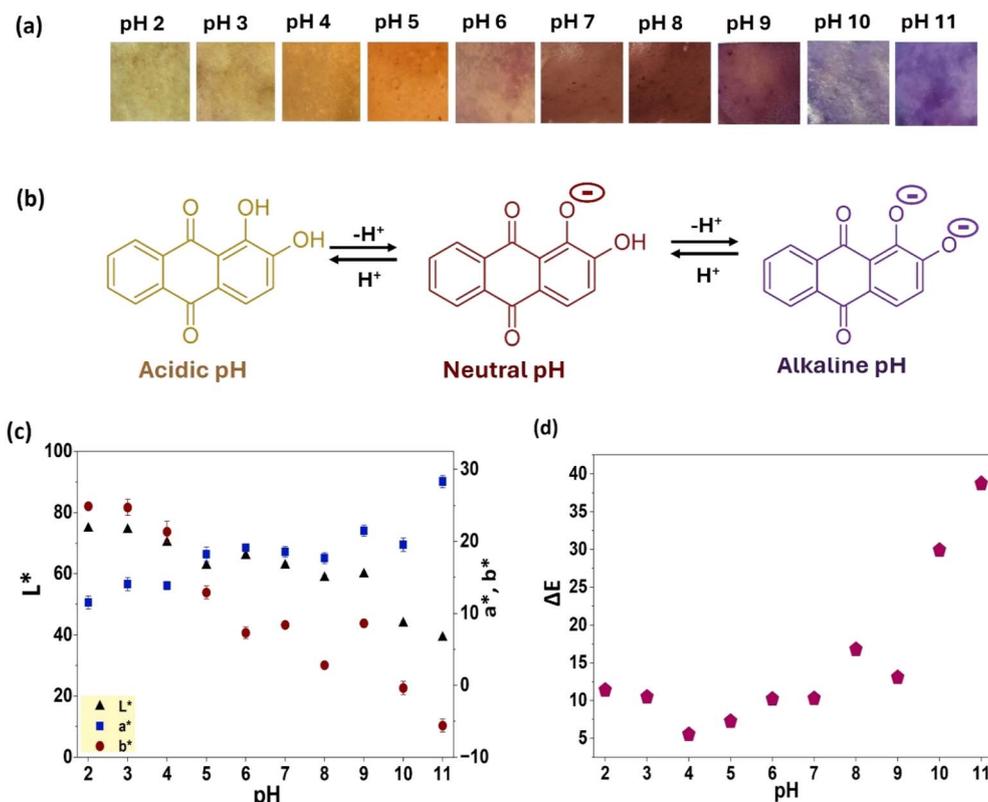
Fig. 8 (a) Photographs of CP/PVA/alizarin indicator at different pH, (b) chemical structure of alizarin under acidic, neutral, and alkaline pH conditions, (c and d) colorimetric parameters of CP/PVA/alizarin indicator at different pH.

lightness of the CP/PVA/alizarin decreased with increasing pH, with the highest (74.8 ± 0.3) and lowest (39.2 ± 0.8) values observed at pH 2 and 11, respectively. This reduction in $L^*$ value implies that the indicator became darker as the pH of the incubating medium increased. Likewise, the $b^*$ value, representing the blueness/yellowness of the indicator, decreased with increasing pH. Notably, the $b^*$ value of the indicator became negative at pH 10, implying a shift from yellow to a bluish hue. This finding is consistent with the purple coloration observed in the digital images of the colorimetric indicator at pH 10 and 11 (Fig. 8a). In contrast, the positive $a^*$ value increased with an increasing pH, with the lowest (11.5 ± 0.9) and highest (28.3 ± 0.5) values observed at pH 2 and 11, respectively. This observation suggests a progressive enhancement in the red hue of the CP/PVA/alizarin indicator with increasing pH. A similar trend in the variation of $L^*$, $a^*$, and $b^*$ values with increasing pH was reported in the literature for the CP/chitosan/alizarin colorimetric indicator.[21] Moreover, the $\Delta E$ of the CP/PVA/alizarin indicator at different pH values from 2 to 11, measured with respect to the as-prepared indicator ($L^* = 68.2 ± 0.2$, $a^* = 15.1 ± 1.1$, and $b^* = 16.4 ± 1.9$), ranged from 5.9 to 38.3, confirming substantial chromatic variation. Overall, both visual observation and quantitative colorimetric analysis demonstrated the excellent pH-sensitive chromatic responsiveness of the CP/PVA/alizarin indicator.

### 3.6. Application of colorimetric indicator in monitoring milk freshness

pH is considered one of the most reliable parameters for evaluating milk freshness in response to microbial growth. During spoilage, lactose, the primary carbohydrate in milk, is metabolized by lactic acid bacteria, resulting in the formation of lactic acid and a subsequent decrease in pH.[4] In general, fresh milk
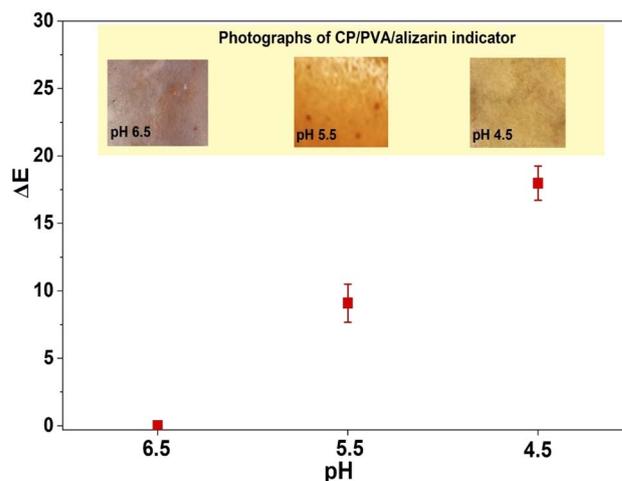


Fig. 9 Photographs and $\Delta E$ of CP/PVA/alizarin indicator incubated in milk of pH 6.5, 5.5, and 4.5.

exhibits a pH in the range of 6–6.8, whereas spoiled milk shows a pH reduction to approximately 4. However, no regulatory authority has yet established a definitive pH threshold to distinguish between fresh and spoiled milk, restricting the standardization of pH-based freshness indicators. In addition to a decrease in pH value, milk spoilage is naturally indicated by the precipitation of milk proteins into solid particles. Specifically, studies in the literature have reported that casein, the predominant milk protein, precipitates around pH 4.5.[4,45] Therefore, in the current work, milk with a pH of 4.5 is considered spoiled.

The $\Delta E$ values and colorimetric responses of the CP/PVA/alizarin indicator tested in milk samples at pH 6.5, 5.5, and 4.5 are presented in Fig. 9. The indicator exhibited a pale brown color for fresh milk (pH 6.5), orange-brown for semi-fresh milk (pH 5.5), and yellow-orange for spoiled milk (pH 4.5) (see inset images in Fig. 9). For colorimetric indicators, a $\Delta E$ above 5 is generally required for the color change to be perceptible to naked eye. From Fig. 9, it can be observed that the $\Delta E$ values of the CP/PVA/alizarin indicator at pH levels of 5.5 and 4.5 are greater than 5, confirming a distinct and visually detectable

color transition associated with milk spoilage. Thus, the CP/PVA/alizarin indicator could be incorporated into milk packaging in a manner that ensures contact with the milk while remaining visible to consumers or automated cameras, enabling spoilage detection without opening the container. Moreover, real-time, non-destructive visual monitoring of milk quality can support retail and consumer decision-making, improve food management, and serve as a reliable tool for minimizing food waste.

### 3.7. Contrast with prior arts

In Table 2, the performance of the CP/PVA/alizarin indicator developed in this study is compared with various pH-responsive colorimetric milk freshness indicators reported in the literature. Weston et al. (2020) developed a polydiacetylene-based milk freshness indicator in which polydiacetylene acted as both the support matrix and the chromogenic component.[4] In another study, Li et al. (2024) reported a milk freshness indicator wherein a polydiacetylene/ZnO nanocomposite served as the chromogenic phase and was immobilized onto

**Table 2** Summary of literature on pH-responsive colorimetric indicators for monitoring milk freshness[a]

| Support materials | Dye/chromogenic component | Fabrication technique | pH sensitivity range | Colorimetric response | Reference |
|---|---|---|---|---|---|
| CP and PVA | Alizarin | Dip coating | 2–11 | Fresh: pale brown Semi-fresh: orange brown Spoiled: yellow orange | This work |
| Polydiacetylene | Polydiacetylene | Solution casting | 1–7 | Fresh: green Semi-fresh: purple Spoiled: pink | 4 |
| Nitrocellulose | Polydiacetylene/ZnO nanocomposite | Immobilization of polydiacetylene/ZnO nanocomposite onto nitrocellulose membrane | 1–7 | Fresh: blue Spoiled: red | 46 |
| Ethylene vinyl alcohol | Bromocresol purple | Chemical functionalization followed by compression moulding | NA | Fresh: green Spoiled: yellow | 47 |
| High-density polyethylene and ethylene-vinyl acetate | Bromothymol blue | Melt mixing followed by compression moulding | NA | Fresh: blue Semi-fresh: bluish-green Spoiled: yellow | 48 |
| Cellulose fibres | Bromocresol purple | Wet laid paper fabrication | 3–9 | Fresh: blue Semi-fresh: cyan Spoiled: yellow | 49 |
| CP | Hibiscus flowers | Rub coating | NA | Fresh: green Semi-fresh: purple Spoiled: pink | 50 |
| CP and starch | Black carrot anthocyanin | Dip coating | 2–11 | Fresh: green Semi-fresh: purple Spoiled: pink | 51 |
| Zein/gelatin | Blueberry anthocyanins | Electrospinning | 3–7 | Fresh: purple-black Semi-fresh: royal purple Spoiled: violet-red | 52 |

[a] NA: Not available.

a nitrocellulose support.[46] Ethylene vinyl alcohol/bromocresol purple[47] and high-density polyethylene/ethylene-vinyl acetate/bromothymol blue[48] indicators have also been investigated for monitoring milk freshness. Although all these indicators demonstrated distinct and perceptible colorimetric responses to milk spoilage, their reliance on non-biodegradable synthetic plastics raises concerns related to food contact safety and plastic pollution. In contrast, the indicator developed in the present study employed CP as the substrate and PVA as the binding agent to enhance dye retention. Both of these materials are biodegradable and biocompatible, making the CP/PVA/alizarin indicator more suitable for safe and environmentally sustainable milk freshness monitoring. Likewise, the synthetic dyes used in ethylene-vinyl alcohol/bromocresol purple, high-density polyethylene/ethylene-vinyl acetate/bromothymol blue, and cellulose fibres/bromocresol purple indicators raise concerns about potential carcinogenic effects on human health.[47–49] In contrast, alizarin, the natural dye incorporated in the present work, has been reported to be safe for food-contact use.[18–20] Moreover, the developed CP/PVA/alizarin indicator exhibited a broad pH-sensitivity range (2–11), comparable to indicators reported using synthetic dyes.[47–49] In addition to producing distinct and perceptible ($\Delta E > 5$) color changes during milk spoilage, alizarin also enhanced antioxidant and UV-blocking properties of the CP/PVA/alizarin indicator, which could potentially contribute to preserving milk quality. Chaithra et al. (2022) reported a milk freshness indicator using CP and a natural dye (hibiscus flowers) that exhibited green, purple, and pink colorimetric responses for fresh, semi-fresh, and spoiled milk, respectively.[50] However, the rub-coating method employed in their study results in weak dye immobilization and poor dye retention, limiting its practical applicability. Similarly, CP/starch/black carrot anthocyanin[51] and zein/gelatin/$Fe^{2+}$/blueberry anthocyanin[52] indicators demonstrated perceptible colorimetric responses distinguishing fresh, semi-fresh, and spoiled milk. Nevertheless, the CP/starch/black carrot anthocyanin indicator exhibited higher water solubility than the CP/PVA/alizarin indicator developed in the present work. Furthermore, these studies did not report properties such as tensile strength, water solubility, and swelling index, which are critical for evaluating dye immobilization, dye retention, and robustness of colorimetric indicators. Overall, this comparative assessment suggests that the CP/PVA/alizarin indicator represents a promising, environmentally sustainable, and multifunctional system with strong potential for reliable real-time monitoring of milk freshness.

## 4 Conclusions

In this work, a novel pH-responsive CP/PVA/alizarin colorimetric indicator for monitoring milk freshness was developed by the dip coating method. FTIR analysis of prepared CP/PVA/alizarin indicator revealed hydrogen bonding interactions between alizarin and the CP/PVA. Meanwhile, FESEM characterization disclosed its compact surface morphology without any phase separation. The water solubility and swelling index of CP/PVA/alizarin are determined to be $9.5 \pm 0.6$ and $77.2 \pm 3.1\%$,

respectively. Compared with neat CP, the CP/PVA/alizarin samples exhibited improved crystallinity (from 69 to 73%), tensile strength (from $5.2 \pm 1.5$ to $37.2 \pm 1.1$ MPa), and elongation at break (from $2.6 \pm 0.5$ to $11.9 \pm 1.1\%$). In addition, the CP/PVA/alizarin demonstrated excellent UV and visible light blocking properties and an outstanding antioxidant activity of $68.3 \pm 3.1\%$. Moreover, it showed color transitions from yellow under acidic pH conditions to reddish-brown at neutral and purple under alkaline pH conditions. Notably, the CP/PVA/alizarin indicator demonstrated its practical potential for monitoring milk freshness through distinct and visually perceivable color transitions ($\Delta E > 5$). Its color changed from pale brown for fresh milk (pH 6.5) to orange-brown for semi-fresh milk (pH 5.5) and yellow-orange for spoiled milk (pH 4.5). While the current study successfully demonstrated the performance of the CP/PVA/alizarin indicator under simulated milk spoilage conditions, further investigations are needed to assess its long-term stability and behavior in real milk storage environments. Accordingly, future research should focus on integrating the CP/PVA/alizarin indicator into conventional milk packaging systems and assessing its performance under varying light, temperature, and mechanical stress conditions to establish its long-term stability and real-time applicability. Furthermore, considering the excellent color sensitivity of the CP/PVA/alizarin indicator across a broad pH range (2–11), it can be explored for monitoring the freshness of other perishable food products such as meat and cheese.

## Author contributions

Satti Venu Gopala Kamari: conceptualization, data curation, analysis, writing – original draft. Jibin Joseph: data curation, analysis, methodology. Kannan Pakshirajan: writing – review & editing. G. Pugazhenthi: conceptualization, resources, supervision, writing – review & editing.

## Conflicts of interest

The authors declare that they have no known competing financial interests or personal relationships that could have appeared to influence the work reported in this paper.

## Data availability

Data will be made available on request.

## Acknowledgements

## References

1 A. N. Mafe, G. I. Edo, R. S. Makia, O. A. Joshua, P. O. Akpoghelie, T. S. Gaaz, A. N. Jikah, E. Yousif,

E. F. Isoje, U. A. Igbuku and D. S. Ahmed, *Food Chem. Adv.*, 2024, **5**, 100852, DOI: 10.1016/j.focha.2024.100852.

2 K. Duan, G. Pang, Y. Duan, H. Onyeaka and J. Krebs, *J. Environ. Manage.*, 2025, **381**, 125246, DOI: 10.1016/j.jenvman.2025.125246.

3 H. Yousefi, H. M. Su, S. M. Imani, K. Alkhaldi, C. D. M. Filipe and T. F. Didar, *ACS Sens.*, 2019, **4**(4), 808–821, DOI: 10.1021/acssensors.9b00440.

4 M. Weston, R. P. Kuchel, M. Ciftci, C. Boyer and R. Chandrawati, *J. Colloid Interface Sci.*, 2020, **572**, 31–38, DOI: 10.1016/j.jcis.2020.03.040.

5 P. Ezati, Y. J. Bang and J. W. Rhim, *Food Chem.*, 2021, **337**, 127995, DOI: 10.1016/j.foodchem.2020.127995.

6 S. Gea, D. Y. Nasution, K. M. Pasaribu, R. M. Tambunan, A. F. Piliang and M. Karina, *S. Afr. J. Chem. Eng.*, 2023, **46**, 277–285, DOI: 10.1016/j.sajce.2023.08.012.

7 H. Shi, L. Wu, Y. Luo, F. Yu and H. Li, *Food Biosci.*, 2022, **48**, 101729, DOI: 10.1016/j.fbio.2022.101729.

8 H. Cheng, H. Xu, D. J. Mc Clements, L. Chen, A. Jiao, Y. Tian, M. Miao and Z. Jin, *Food Chem.*, 2022, **375**, 131738, DOI: 10.1016/j.foodchem.2021.131738.

9 G. Xia, Y. Ma, Q. Ma, X. Yao, Z. Xu, X. Ji and F. Zhang, *Food Packag. Shelf Life*, 2024, **46**, 101413, DOI: 10.1016/j.fpsl.2024.101413.

10 F. E. Tirtashi, M. Moradi, H. Tajik, M. Forough, P. Ezati and B. Kuswandi, *Int. J. Biol. Macromol.*, 2019, **136**, 920–926, DOI: 10.1016/j.ijbiomac.2019.06.148.

11 S. Huang, Y. Xiong, Y. Zou, Q. Dong, F. Ding, X. Liu and H. Li, *Food Hydrocolloids*, 2019, **90**, 198–205, DOI: 10.1016/j.foodhyd.2018.12.009.

12 F. S. Mohseni-Shahri and F. Moeinpour, *Food Sci. Nutr.*, 2023, **11**(7), 3898–3910, DOI: 10.1002/fsn3.3375.

13 J. Goudarzi, H. Moshtaghi and Y. Shahbazi, *Food Packag. Shelf Life*, 2023, **35**, 101017, DOI: 10.1016/j.fpsl.2022.101017.

14 F. Fakhrghasemi, N. Shavisi, Y. Shahbazi, H. Yousefi and A. Ullah, *Food Bioprocess Technol.*, 2025, **18**(10), 8861–8879, DOI: 10.1007/s11947-025-03947-x.

15 Y. Deng, Z. Li, S. Wu, H. Zheng, H. Lei, X. Ge and Z. Guo, *Int. J. Biol. Macromol.*, 2025, **308**, 142040, DOI: 10.1016/j.ijbiomac.2025.142040.

16 Y. Mohammadi, Y. Shahbazi and N. Shavisi, *LWT-Food Sci. Technol.*, 2024, **208**, 116707, DOI: 10.1016/j.lwt.2024.116707.

17 Y. Khaledian, H. Moshtaghi and Y. Shahbazi, *Food Chem.*, 2024, **434**, 137462, DOI: 10.1016/j.foodchem.2023.137462.

18 Y. Liu, H. Li, J. Chen, J. Feng, R. Lian, L. Fu and Y. Wang, *J. Funct. Foods*, 2024, **4**(2), 135–141, DOI: 10.1016/j.jfutfo.2023.06.004.

19 Y. Zou, S. Chen, H. Dou, W. Zhu, D. Zhao, Y. Wang, H. Wang and X. Xia, *Food Packag. Shelf Life*, 2024, **42**, 101249, DOI: 10.1016/j.fpsl.2024.101249.

20 P. Ezati, J. W. Rhim, M. Moradi, H. Tajik and R. Molaei, *Carbohydr. Polym.*, 2020, **246**, 116614, DOI: 10.1016/j.carbpol.2020.116614.

21 P. Ezati, H. Tajik and M. Moradi, *Sens. Actuators, B*, 2019, **285**, 519–528, DOI: 10.1016/j.snb.2019.01.089.

22 P. Ezati and J. W. Rhim, *Food Hydrocolloids*, 2020, **102**, 105629, DOI: 10.1016/j.foodhyd.2019.105629.

23 P. Ezati, H. Tajik, M. Moradi and R. Molaei, *Int. J. Biol. Macromol.*, 2019, **132**, 157–165, DOI: 10.1016/j.ijbiomac.2019.03.173.

24 D. Zhang, Q. Shu and Y. Liu, *J. Food Prot.*, 2024, **87**(10), 100339, DOI: 10.1016/j.jfp.2024.100339.

25 Z. Jiang and T. Ngai, *Polymers*, 2022, **14**(8), 1533, DOI: 10.3390/polym14081533.

26 K. Muthamma and D. Sunil, *ACS Omega*, 2022, **7**(47), 4268–42699, DOI: 10.1021/acsomega.2c05547.

27 X. Zhang, W. Liu and C. Li, *Int. J. Biol. Macromol.*, 2024, **282**, 137329, DOI: 10.1016/j.ijbiomac.2024.137329.

28 M. Ziyaina, B. Rasco and S. S. Sablani, *Food Control*, 2020, **110**, 107008, DOI: 10.1016/j.foodcont.2019.107008.

29 A. Khan, P. Ezati and J. W. Rhim, *Colloids Surf., B*, 2023, **223**, 113169, DOI: 10.1016/j.colsurfb.2023.113169.

30 S. V. G. Kumari, S. P. A. Gupta, K. Pakshirajan and G. Pugazhenthi, *Polym. Eng. Sci.*, 2023, **63**(11), 3855–3864, DOI: 10.1002/pen.26491.

31 D. Liu, C. Zhang, Y. Pu, S. Chen, H. Li and Y. Zhong, *Food Chem.*, 2023, **404**, 134426, DOI: 10.1016/j.foodchem.2022.134426.

32 S. V. G. Kumari, S. Rawat, D. Vasanth, R. B. Valapa, K. Pakshirajan and G. Pugazhenthi, *Polym. Eng. Sci.*, 2025, **65**(5), 2455–2467, DOI: 10.1002/pen.27160.

33 S. V. G. Kumari, K. Pakshirajan and G. Pugazhenthi, *Int. J. Biol. Macromol.*, 2023, **252**, 126566, DOI: 10.1016/j.ijbiomac.2023.126566.

34 F. T. Moreira, B. P. Correia, M. P. Sousa and G. F. Sales, *Microchim. Acta*, 2021, **188**(10), 334, DOI: 10.1007/s00604-021-04996-7.

35 S. S. Ma and Y. G. Zhang, *Environ. Sci. Pollut. Res.*, 2016, **23**(22), 22771–22782, DOI: 10.1007/s11356-016-7483-6.

36 M. M. El-Nahass, H. M. Zeyada, N. A. El-Ghamaz and A. S. Awed, *Optik*, 2018, **170**, 304–313, DOI: 10.1016/j.ijleo.2018.05.130.

37 H. N. Abdelhamid and A. P. Mathew, *Carbohydr. Polym.*, 2021, **274**, 118657, DOI: 10.1016/j.carbpol.2021.118657.

38 N. Thungphotrakul and P. Prapainainar, *Int. J. Biol. Macromol.*, 2024, **282**, 137223, DOI: 10.1016/j.ijbiomac.2024.137223.

39 S. Tanpichai, Y. Srimarut, W. Woraprayote and Y. Malila, *Int. J. Biol. Macromol.*, 2022, **213**, 534–545, DOI: 10.1016/j.ijbiomac.2022.05.193.

40 Y. He, H. Li, X. Fei and L. Peng, *Carbohydr. Polym.*, 2021, **252**, 117156, DOI: 10.1016/j.carbpol.2020.117156.

41 S. E. Duncan and S. Hannah, *Emerg. Food Packag. Technol.*, 2012, 303–322, DOI: 10.1533/9780857095664.3.303.

42 A. Manzoor, B. Yousuf, J. A. Pandith and S. Ahmad, *Food Biosci.*, 2023, **53**, 102717, DOI: 10.1016/j.fbio.2023.102717.

43 H. Zhang, M. Li, Z. Liu, R. A. Li and Y. Cao, *Int. J. Biol. Macromol.*, 2024, **275**, 133535, DOI: 10.1016/j.ijbiomac.2024.133535.

44 R. Priyadarshi, P. Ezati and J. W. Rhim, *ACS Food Sci. Technol.*, 2021, **1**(2), 124–138, DOI: 10.1016/j.ijbiomac.2024.133535.

45 M. Lu and N. S. Wang, *Microbiol. Qual. Food*, 2017, 151–178, DOI: 10.1016/b978-0-08-100502-6.00010-8.

46 Z. Li, H. Jang, S. Park, S. M. Kim and T. J. Jeon, *Biotechnol. Bioprocess Eng.*, 2024, **29**(1), 177–183, DOI: 10.1007/s12257-024-00021-9.

47 L. R. Magnaghi, C. Zanoni, G. Alberti, P. Quadrelli and R. Biesuz, *Talanta*, 2022, **241**, 123230, DOI: 10.1016/j.talanta.2022.123230.

48 M. K. Stocker, M. L. Sanson, A. A. Bernardes, A. M. Netto and R. Brambilla, *J. Sol-Gel Sci. Technol.*, 2021, **98**(3), 568–579, DOI: 10.1007/s10971-021-05529-7.

49 R. Liu, W. Chi, Q. Zhu, H. Jin, J. Li and L. Wang, *Foods*, 2023, **12**(9), 1857, DOI: 10.3390/foods12091857.

50 K. P. Chaithra and T. P. Vinod, *ChemistrySelect*, 2022, **7**(41), e202201839, DOI: 10.1002/slct.202201839.

51 M. M. Goodarzi, M. Moradi, H. Tajik, M. Forough, P. Ezati and B. Kuswandi, *Int. J. Biol. Macromol.*, 2020, **153**, 240–247, DOI: 10.1016/j.ijbiomac.2020.03.014.

52 R. Gao, H. Hu, T. Shi, Y. Bao, Q. Sun, L. Wang, Y. Ren, W. Jin and L. Yuan, *Curr. Res. Food Sci.*, 2022, **5**, 677–686, DOI: 10.1016/j.crfs.2022.03.016.